Proceedings of First International Conference on Smart Systems and Green Energy Technologies (ICSGET 2022)

Design and study of a double – boost non-isolated converter with continuous input current

[1]A. Gopalakrushna, [2]G. Priyanka

[1,2]Department of EEE, Vignana Bharathi Institute of Technology, Hyderabad, India
Email: agopalakrushna@gmail.com, gpriyanka4598@gmail.com

Abstract

Environmental pollution is becoming worse, and the energy issue is getting worse. New electric vehicles (NEVs), on the other hand, are drawing steadily greater attention. DC – DC converters are therefore necessary in electric vehicle applications to obtain high voltage gain and improved power regulation. Therefore, investigation on high voltage gain DC – DC configurations is quite crucial. The study on double-boost DC – DC configuration with continuous input current and high gain is proposed in this project. The suggested converter also enhances efficiency while resolving switching stress and output voltage ripple issues. With fewer parts, a straightforward design, and the aforementioned benefits, the double boost converter will be a serious rival to existing high gain converters. Utilizing the MATLAB/SIMULINK software, a simulation design was created to demonstrate the viability of the suggested converter. To demonstrate the performance's robustness and functioning capacity, it is also evaluated under various duty ratios.

Keywords. Double-boost, continuous input current, non-isolated, dc – dc configuration.

1. INTRODUCTION

New energy vehicles, sometimes referred to as NEVs, are garnering an increasing amount of interest as ecological contamination and the energy emergency continue to worsen. Ultra-gain DC-DC topologies may be split into several separate categories, each of which is defined by the topologies that they utilize and the applications that they are meant to fulfil. Ultra-gain DC-DC topologies can be found in a variety of different applications. Depending on whether or not a transformer is used in the design, they can either be nonisolated DC-DC configurations or isolated DC-DC configurations [1]. These converters fall into one of two categories. A nonisolated DC-DC converter provides a number of benefits, some of which include a high-power density, an uncomplicated design, and an easy-to-understand and straightforward control. Because of the transformer, the isolated converter suffers from a variety of drawbacks, the most significant of which are its substantial bulk, its small power density, and its straightforward magnetic flux saturation. Because of these drawbacks, the implementation of isolated structures in electric vehicle

e-ISBN: 9788770229647 https://doi.org/10.13052/rp-9788770229647.013

(EV) applications can be restricted. So, nonisolated DC-DC configurations are recommended for the overhead applications to get the most power density and efficiency [2].

The vast majority of hybrid topologies in research on the topology of nonisolated DC-DC configurations use expansions of fundamental chopper circuits. These topologies are used because they are the most efficient. Cascaded topologies, topologies that are based on Z-source & quasi-Z-source, switched capacitor and switched inductor configurations are some examples of these types of topologies. There is a DC-DC converter with a high voltage gain that was derived from a Zeta converter. Even though there is only one primary switch in the design, utilizing a switching mode that has a low resistance can assist in decreasing switching loss in addition to voltage stress. This is because low resistance allows for a smoother transition between states. In [3], high voltage gain, a non-coupled inductor, SEPIC-based DC-DC converter was demonstrated to the audience. This converter eliminates the need for an extra clamping circuit and reduces the amount of conductive loss that occurs as a result of its utilization of a switch that possesses lower levels of conductive resistance. This converter has several benefits, some of which include an output voltage that is in-phase, high efficiency, a high voltage gain, a stable input current, and reduced voltage stress. Other advantages include the same. A DC - DC converter with a large voltage gain is described. This converter combines the most useful aspects of a cuk converter and a secondary boost into a single piece of equipment for your convenience. This converter needs just one switch in order to accomplish the goals of having a high step-up ratio, having streamlined control, and having common ground on both the input and output sides.

In the research described in reference number [4], a voltage multiplier converter was developed that made use of switched capacitors. This specific boost converter has a boost ratio that is twice as high as that of regular boost topologies, yet the voltage stress that it exerts on capacitors and diodes is only half as severe as the stress that is caused by the typical boost converters. Another issue is that there is a mismatch between the data that is being input and the data that is being produced. Cascade design may be utilized in a variety of applications, including fuel cells. The first stage of this design is made up of two boost converters that are staggered in different directions. The second step of this architecture is a three- level boost converter. Both the interleaved structure and the three-level design have the potential to lessen the ripple in the input current. However, only the three-level architecture can minimize switching loss and increase converter efficiency. It is feasible to enjoy both of these benefits at the same time. This is despite the fact that the voltage gain has not changed. An input that is made up of four parallel connections between inductors is included in a DC/DC converter that has four phases that interleave with each other. This helps to smooth out the waveforms. As a consequence, the total value of the ripple effect is diminished. Particle swarm optimization is an example of an optimization strategy. The system is optimized by the use of a particle swarm with this method. The results of the studies show that

e-ISBN: 9788770229647 https://doi.org/10.13052/rp-9788770229647.013

the suggested method of control is better in terms of both how well it works and how well it can be tracked and changed [5].

Particle swarm optimization and artificial physical optimization are used in the research work to achieve the goals of vector decoupling and parameter tweaking in the context of an electric car charging system. These goals were successfully attained. Validation of a system that uses tools that include hardware in the loop can be accomplished by using a boost converter that is of the standard bidirectional kind. The results of the experiment back up the idea that the suggested method is both reliable and effective. This strategy is proposed as a possible solution. The objective of this strategy is to modify the electric grid in such a way that it makes use of alternative and renewable forms of energy in order to facilitate the rapid recharging of electric cars. In the publication [6], the authors recommend the use of an endless series input boost converter that possesses a high fault tolerance for scenarios that involve vehicle-to-aid communication. The outcomes of a series of experiments that compared the performance. The results of this study were achieved through a process of experimental comparison.

In conclusion, hybrid topologies are formed by employing fundamental DC-DC converters, which are then paired with switched inductors or switched capacitors [7,8]. In addition, hybrid topologies can also use switched resistors. Although this may combine the benefits of numerous distinct topologies, the negatives of each of the various topologies that it combines are still very important. This is the case even though Z-source converters have the potential to significantly increase the voltage gain. This paper is organised into four sections, Section II describes about the propose converter circuit configuration and its analysis in the CCM mode. In Section III the simulation block diagram and results are given a detailed discussion is done. Finally, conclusions are made in section IV.

2. DOUBLE-BOOST CONFIGURATION

Figure 1 depicts the proposed double-boost configuration. The configuration is comprised of 3 diodes D1, D2, & D3, 2 power switches Q1 & Q2, 2 inductors L1 & L2, and a capacitor that acts as an output filter. Q1 & Q2 are the power switches. If the inductors L1 & L2 are the identical, then the enduring diodes and MOSFET switches will have the same characteristics. Figures 2 and 3 illustrate the two distinct ways in which the converter can perform its job.

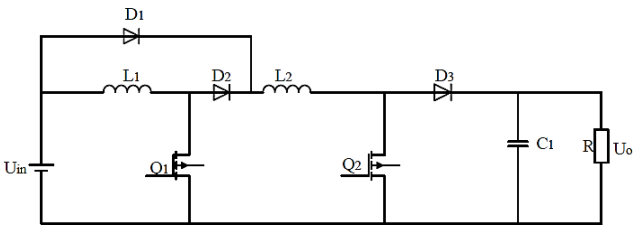

Figure 1. Double-boost circuit configuration

e-ISBN: 9788770229647 https://doi.org/10.13052/rp-9788770229647.013

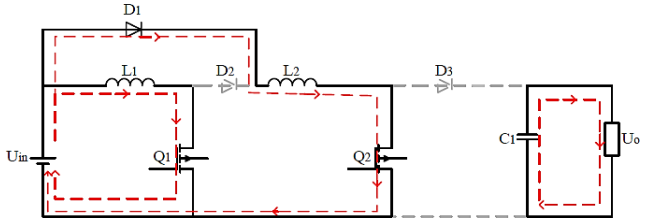

Figure 2 Switch ON

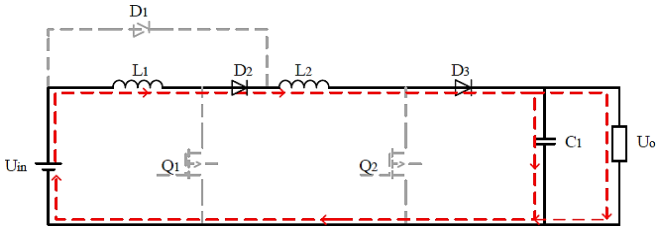

equivalent circuit

Figure 3. Switch OFF equivalent circuit

In the ON period, the power supply charges the inductors L1 and L2, and the inductors charges the energy; the C1 capacitor transfers the energy to the resistance. Indicating that the converter is in the ON state is the simultaneous activation of switches Q1 and Q2. Figure 2 depicts the operating mode that will be utilized by the proposed converter. During this time, the diode D1 is active while the diodes D2 and D3 are active with the voltage in the opposite direction. The first loop is produced when the input power Uin begins to charge the inductor L1, which does so by way of the switch Q1. The input power Uin is responsible for charging the inductor L2 via the switch Q2. The load gets power from the output capacitor C1. The equation (1) below demonstrates the amount of energy.

$$W_L = U_{in} I_L D T_S \quad (1)$$

In this equation, WL stands for the amount of energy that is taken in by the inductor during the time that the switch is turned on. In the OFF state of the analogous circuit, when both switches Q1 and Q2 are closed, energy from the input power supply flows via L1 and L2 inductors and charges capacitor C1. Figure 3 displays the converter's active mode. In this mode, the reverse voltage causes diodes D2 and D3 to switch off, while it causes diode D1 to turn on. The input energy supply Uin & the L1 and L2 inductors are joined in series with one another in order to give power to the resistance plus charges the filter capacitor C1. The amount of energy may be seen in equation 2.

$$W_L' = \left(\frac{U_o - U_{in}}{2}\right) \times I_L \times (1 - D) \times T_S \quad (2)$$

e-ISBN: 9788770229647 https://doi.org/10.13052/rp-9788770229647.013

where WL' is the amount of energy that is created by the inductor during the time that the switch is turned off and 1-D is the amount of time that the switch is turned on. The law of energy conservation may be used to derive the below equation, which can be constructed as Equation based on the rule (3).

$$W_L = W_L' \tag{3}$$

In accordance with Equations (1) through (3), the voltage conversion ratio G (D) of the given topology may be calculated in Equation (4).

$$G_D = \frac{1+D}{1-D} \tag{4}$$

3. SIMULATION RESULTS

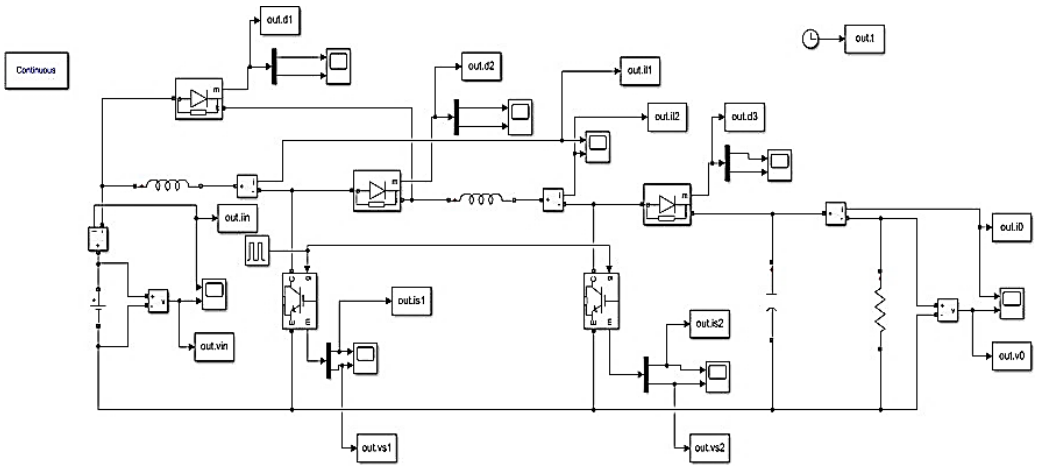

Figure 4. Simulation model of Double Boost DC-DC Configuration

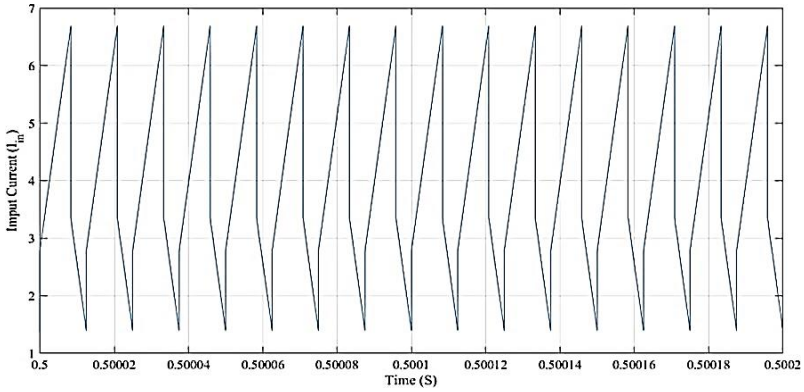

Figure 5. Simulation waveform of input current

e-ISBN: 9788770229647 https://doi.org/10.13052/rp-9788770229647.013

A simulation platform, depicted in Fig. 4, was developed to validate its performance. The projected converter is designed for an output power of 200W, with an output voltage of 250V. With the input voltage of 50V, the required output can be produced at a duty ratio of 66.67%. The load is calculated as 312.5Ω. For the simulation 80 kHz frequency is considered. The waveform shown in the fig 5 represents the change in input with respect to time. As the input current is continuous with an allowable ripple. Figure 6 represents the input DC voltage waveform plotted using MATLAB simulation. A 50V DC input voltage is considered as the input to design the proposed converter which can be observed in fig. 6. The output power and voltage are considered randomly for the design.

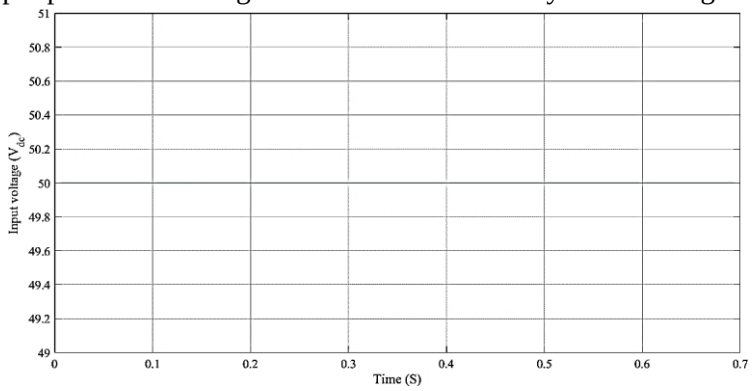

Figure 6. Simulated waveform of input voltage

The simulated output waveforms are shown in the figs. 7 & 8 of the proposed integrated converter. For a 200 W power, the integrated converter is designed with an output voltage of 250V. A load of 312.5Ω resistance is used at the output and hence the DC output current can be given as 0.8A theoretically.

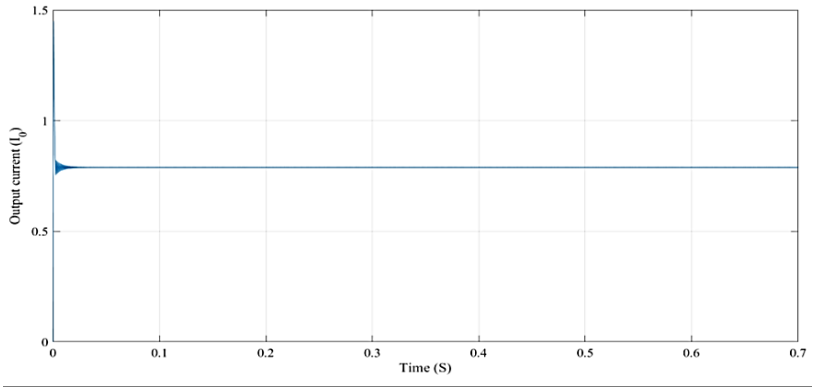

e-ISBN: 9788770229647 https://doi.org/10.13052/rp-9788770229647.013

Figure 7. Simulation waveform of output current

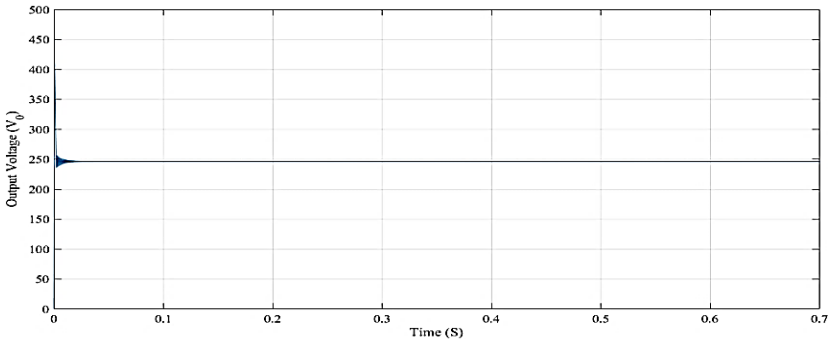

Figure 8. Simulation waveform of output voltage

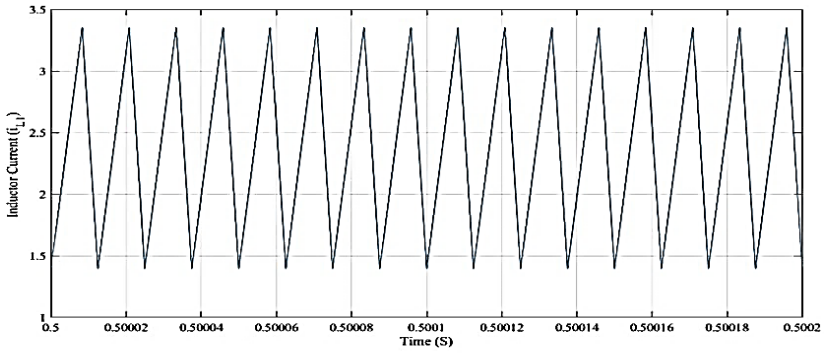

Figure 9. Simulation waveform of inductor current $I_{L1.}$

Figure 7 shows the simulated output current waveform with negligible ripple. The simulated value is approximately 0.75A and is much closed to the computed theoretical value. Figure 8 represents the simulated DC output voltage waveform with very low ripple (<0.5% approximately). The simulated value is approximately 247V and is much closed to the computed theoretical value. Figures 9 & 10 shows the simulated inductor current waveforms i_{L1}& i_{L2} respectively (for 16 cycles). From fig. 9 it can be noted that the inductor L_1 peak to peak ripple approximately 2A. This value is exactly matches to the theoretical consideration of inductor L_1 design. From fig. 10 it can be noted that the inductor L_2 peak to peak ripple approximately 2A. This value is exactly matches to the theoretical consideration of inductor L_2 design. For various duty ratios the proposed converter shows better performances with an efficiency greater than 90.

e-ISBN: 9788770229647 https://doi.org/10.13052/rp-9788770229647.013

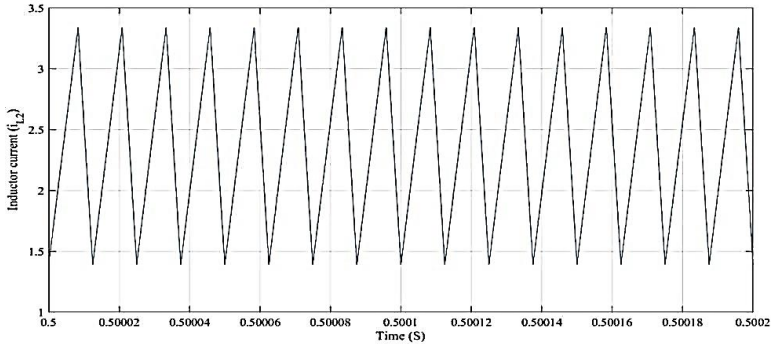

Figure 10. Simulation waveform of inductor current I_{L2}

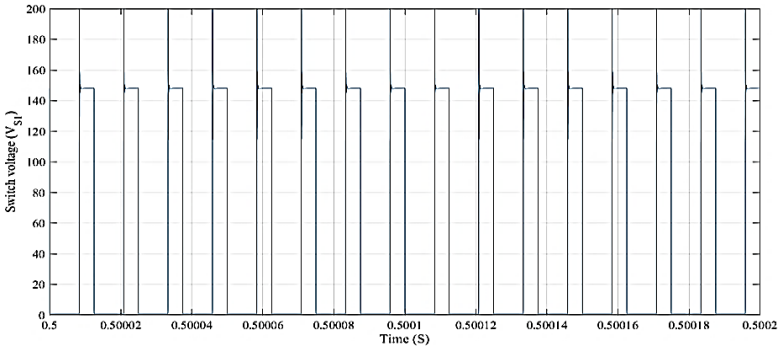

Figure 11. Plot of Switch voltage V_{s1}

The simulation waveform of switch voltage Vs1 is shown in fig. 11, during the time interval of 0.50002s. The waveform shows the switch voltage at 150V, with respect to time. The simulation waveform of switch current Is1 is shown in fig 4.12, during the time interval of 0.50002s. The waveform shows the switch current at 3.4 amps with respect to time.

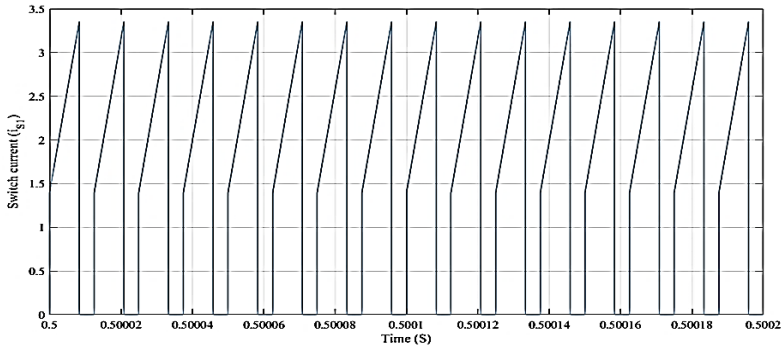

e-ISBN: 9788770229647 https://doi.org/10.13052/rp-9788770229647.013

Figure 12. Plot of Switch current I_{s1}

Figure 13. Plot of Switch voltage V_{s2}

The simulation waveform of switch voltage Vs2 is shown in fig.13, during the time interval of 0.50002s. The waveform shows the switch voltage at 245V, with respect to the time. The simulation waveform of switch current Is2 is shown in fig.14, during the time interval of 0.50002s. The waveform shows the switch current at 3.3 amps with respect to the time.

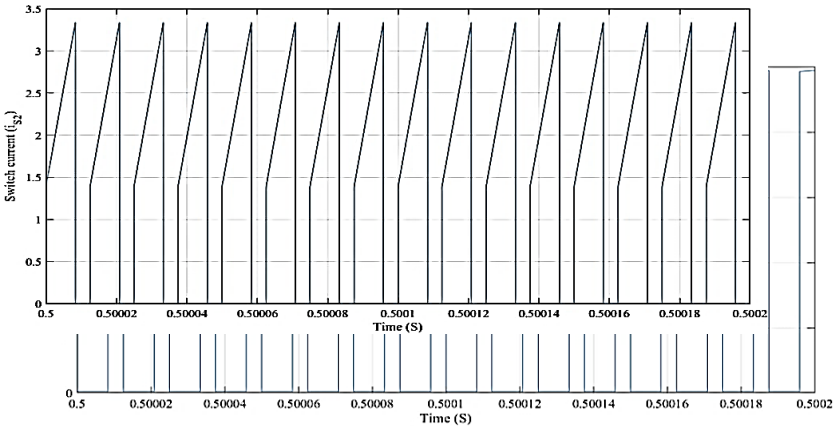

Figure 14. Plot of Switch current I_{s2}

4. CONCLUSION

From an investigation into the working principle of the proposed converter, as well as its modelling, the results of proposed DC-DC converters, which are frequently utilized in electric vehicles, one can derive the following conclusions:

1. When compared to standard boost configurations the converter that was presented offers a number of advantages, particularly in terms of the voltage gain, the device stress, and the number of components.
2. It may quicken the return of the output voltage to stability when there is a sudden change in the load and the input voltage.
3. Under a wide range of conditions, the double converter that was recommended provides glaring benefits in terms of both the real voltage conversion ratio and the efficiency of the system.
4. In addition, in contrast to the usual boost configuration, the double-boost network that was suggested has a lower ripple in output voltage.

REFERENCES

1. Ali, A.; Hossein, A.; Amir, F. A novel high step-up DC/DC converter based on integrating coupled inductor and switched-capacitor techniques for renewable energy applications. IEEE Trans. Power Electron. 30, 4255– 4263, 2015.

e-ISBN: 9788770229647 https://doi.org/10.13052/rp-9788770229647.013

2. Nagi reddy. B, Sahithi Priya. Kosika, Manish patel. Gadam, jagadhishwar. Banoth, Ashok. Banoth, Srikanth goud. B, "Analysis of positive output buck-boost topology with extended conversion ratio", Journal of Energy Systems, 6(1), pp. 62–83, 2022.
3. Arab, A.S, Shokrollahi, M.J. A novel high voltage gain noncoupled inductor SEPIC converter, IEEE Trans. Ind Electron, 66, 7099–7108, 2019
4. Yun, Z.; Lei, Z.; Mark, S.; Ping, W. Single-Switch, Wide Voltage-Gain Range, Boost DC–DC Converter for Fuel Cell Vehicles. IEEE Trans. Veh. Technol. 2018, 67, 134–145.
5. Vinnikov, D.; Roasto, I.; Strzelecki, R.; Adamowicz, M. Step-Up DC/DC Converters with Cascaded Quasi-Z-Source Network. IEEE Trans. Ind. Electron. 2012, 59, 3727–3736.
6. Rodríguez Licea, M.A. Fault Tolerant Boost Converter with Multiple Serial Inputs and Output Voltage Regulation for Vehicle-to-Aid Services. Energies, 13, 1694, 2020.
7. Nagi Reddy, B., Pandian, A., Chandra Sekhar, O., Ramamoorty, M. "Performance and dynamic analysis of single switch AC-DC buck-boost buck converter" International Journal of Innovative Technology and Exploring Engineering, 2019, 8(4), pp. 307–313.
8. Nagi Reddy, B., Chandra Sekhar, O., Ramamoorty, M. "Analysis and implementation of single-stage buck-boost-buck converter for battery charging applications Journal of Advanced Research in Dynamical and Control Systems, 2018, 10(4), pp. 446–457.

e-ISBN: 9788770229647 https://doi.org/10.13052/rp-9788770229647.013